

A Hybrid Time-Stepping Scheme for Intermittent Contact in Multi-Rigid-Body Dynamics

Kishor D. Bhalerao* Kurt S. Anderson†

Jeffrey C. Trinkle‡

Rensselaer Polytechnic Institute, Troy NY 12180

Abstract

This paper describes a novel method for the modeling of intermittent contact in multi-rigid-body problems. We use a complementarity based time-stepping scheme in Featherstone's Divide and Conquer framework to efficiently model the unilateral and bilateral constraints in the system. The time-stepping scheme relies on impulse-based equations and does not require explicit collision detection. A set of complementarity conditions is used to model the interpenetration constraint and a linearized friction cone is used to yield a linear complementarity problem. The Divide and Conquer framework ensures that the size of the resulting mixed linear complementarity problem is independent of the number of bilateral constraints in the system. This makes the proposed method especially efficient for systems where the number of bilateral constraints are much greater than the number of unilateral constraints. The method is demonstrated by applying it to a falling 3D double pendulum.

1 Introduction

Modeling of unilateral constraints in a system of interconnected bodies is a frequently encountered problem in the design and optimization of simple mechanisms, robotic manipulators, automobiles, manufacturing assemblies and complex spacecrafts. Accurate simulation models reduce the time and cost associated with the design, prototyping and testing of such engineering systems while improving their performance.

In real-world applications, local deformations are expected to occur at all the unilateral contacts. Traditionally, there are two different strategies to model these intermittent contacts. The first approach is to model the local deformation on contacting bodies [1] with the normal and tangential interaction forces between the contacting bodies being determined from a local deformation model. These forces in turn influence the dynamic behavior of the system. The advantage of this approach is that the system of equations is effectively

*Email:bhalek@rpi.edu, Department of Mechanical, Aerospace and Nuclear Engineering

†Email:anderk5@rpi.edu, Department of Mechanical, Aerospace and Nuclear Engineering

‡Email:trink@cs.rpi.edu, Department of Computer Science

a set of PDE's and in theory may be solved by conventional methods. The disadvantage of this kind of approach is the difficulty of developing and analyzing a good local contact/deformation model. Additionally, such formulations are inclined to produce very stiff systems of equations which are computationally expensive to solve. Such treatments capture local dynamic behavior in and around the contact site which often exists at sufficiently small spatial and temporal scales relative to that of the primary motion of the system as to be of no interest. Unfortunately, it is this unimportant local dynamic response which governs the behavior of the temporal integration of the system equations resulting in unacceptably slow and computationally expensive simulations. For example modeling metal-metal contacts in this manner, as one might find in certain tracked vehicle problems, often leads to integration steps of less than 10^{-6} seconds in order to maintain integrator stability while the temporal scale of interest is usually several orders higher (e.g 10-20 seconds) than the integrator time step. This happens because the local force-deformation model has captured the ringing of the metal. This ringing can be eliminated by replacing the local stiff deformation model with a kinematic constraint. Thus, it is often desirable to ignore the localized deformations of the interacting bodies and treat them as rigid.

This points to the other important strategy which does not consider local deformations but instead focuses on kinematic constraints and impulsive changes in the state [2]-[7]. The contact process is governed by a set of complementarity rules also known as Signorini's law. It states that in contact dynamics either relative normal kinematical quantities are zero and the accompanying constraint forces or constraint force combinations are not zero, or vice versa. For a closed contact the relative normal distance and normal velocity of the colliding bodies are zero and the constraint force in the normal direction is not zero, or the reciprocal. The exception to the above rules is the special case when both the normal relative kinematical quantities and the associated constraint forces are simultaneously zero. For stiction the tangential relative velocity is zero, and the constraint force is located within or on the boundary of the friction cone. The resulting inequalities are then used for an evaluation of the transitions between the contact states. In the traditional approach, a multibody system with m_B bilateral constraints and m_U unilateral constraints results in an expensive $O(2^{m_U})$ combinatorial problem (Briefly discussed in section 2) of determining a consistent set of contact states [6]. The use of complementarity methods significantly alleviates this $O(2^{m_U})$ combinatorial process by extending the contact laws to unambiguously describe transitions for all possible contact states and generate only consistent contact state sets. This kind of an approach was employed by Moreau [8] and extended by others [4]-[7],[9]-[14].

For a multibody system the overall complexity is characterized by the number of generalized coordinates (n) and active constraints (m) which are bilateral constraints (m_B) and unilateral constraints (m_U). In this respect, the straight forward application of classical multibody methods (Newton-Euler and Lagrange) commonly require $O(n^3)$ computations to construct the system-wide mass matrix and solve for the accelerations at each time step. For highly constrained systems, this can be prohibitive. Alternatively such systems may be described as a set of differential algebraic equations (DAEs), which are as a rule sparse and of near maximal dimension and must utilize special sparse system solvers and integration schemes.

This paper describes a hybrid *Divide and Conquer-Complementarity* approach to efficiently model the unilateral and bilateral constraints in multibody systems. This hybrid

formulation is felt to offer some advantages over the classical approach to model unilateral constraints since the Divide and Conquer Algorithm (DCA) [15, 16, 17] does not require building a system mass matrix to compute the generalized accelerations for the system and the use of *Complementarity Method* on an average avoids the expensive $O(2^{mv})$ combinatorial problem of determining consistent contact states. The complementarity solvers may still incur an exponential expense in the worst case scenarios. However, in most cases, they produce a solution significantly faster.

The outline of the paper is as follows. First a brief discussion of the classical approach to model unilateral constraints in multibody dynamics is presented. This is followed by the description of the complementarity based contact model and the time stepping scheme for a single body. The paper then describes how this model can be used for unilateral constraints in a DCA framework for a general multibody system. The paper then concludes by giving numerical results for a free falling 3D double pendulum on a plane with friction and a comparison with an Autolev model.

2 Traditional Complementarity Based Approach for Multibody Problems

A standard Linear Complementarity Problem (LCP) can be defined as follows. For a given matrix $A_1(n \times n)$ and vector $b_1(n \times 1)$, find a $n \times 1$ vector z such that the following conditions are satisfied.

$$w = A_1 z + b_1, \quad (1)$$

$$0 \leq w \perp z \geq 0. \quad (2)$$

We get a Mixed Complementarity Problem (MCP) if there are additional equality constraints on z of the form $\mathbf{0} = A_2 z + b_2$, where A_2 and b_2 are known and of dimensions $m \times n$ and $m \times 1$, respectively. The interested reader can find a detailed discussion on LCP and MCP in [18]. The goal is then to cast the equations describing the unilateral constraints into a LCP (or MCP).

The equations of motion for a general multibody system can be expressed in the following standard form.

$$\underline{u} = \underline{Y}(q, t)\underline{\dot{q}} + \underline{Z}(q), \quad (3a)$$

$$\underline{K}(q, \underline{\dot{q}}, t) = \underline{M}(q, t)\underline{\dot{u}} + \underline{A}^T(q, t)\underline{\lambda}, \quad (3b)$$

$$\underline{\Phi}(q, \underline{\dot{q}}, t) = \underline{0}. \quad (3c)$$

In these equations, $q_{n \times 1}$ represents the n generalized system coordinates and the associated time derivatives or the generalized speeds are represented by \underline{u} . Equation (3a) maps $\underline{\dot{q}}$ into generalized speeds \underline{u} which are velocity level quasi-coordinates that facilitate the formulation. The matrix \underline{M} is the system mass matrix, while \underline{K} consists of all the forcing terms which are state dependent, such as external forces and body forces, and additionally includes the inertia forces arising from the centripetal and Coriolis accelerations. The quantity \underline{A} is the

constraint Jacobian associated with the partial derivative of the m independent algebraic constraint equations represented by equation (3c) with respect to \underline{q} and \underline{u} .

In general this system may have a total of m_B bilateral and m_U unilateral constraints. Whenever a unilateral constraint becomes active it restricts the relation between certain degrees of freedom for the system. A direct consequence is that the effective degrees of freedom for the system vary depending upon its state and the number of active unilateral constraints. Correct representation of contact states requires appropriately enforcing the unilateral constraints on the system. The admissible motions of each body in the system which are compatible with kinematic constraints necessary to represent contact states have been described in [3]. These can be expressed as follows.

$$\dot{\underline{g}}_{N(m_N \times 1)} = \underline{W}_N^T \underline{u} + \tilde{\underline{w}}_N \quad , \quad \dot{\underline{g}}_{T(m_T \times 1)} = \underline{W}_T^T \underline{u} + \tilde{\underline{w}}_T, \quad (4)$$

$$\ddot{\underline{g}}_{N(m_N \times 1)} = \underline{W}_N^T \dot{\underline{u}} + \dot{\underline{W}}_N^T \underline{u} + \bar{\underline{w}}_N, \quad (5)$$

$$\ddot{\underline{g}}_{T(m_T \times 1)} = \underline{W}_T^T \dot{\underline{u}} + \dot{\underline{W}}_T^T \underline{u} + \bar{\underline{w}}_T. \quad (6)$$

Where $\underline{g}_{N(m_N \times 1)}$ represents the normal distances at the points of potential contact. $\dot{\underline{g}}_{N(m_N \times 1)}$ and $\dot{\underline{g}}_{T(m_T \times 1)}$ are the normal and tangential components of the relative velocities, and the corresponding relative accelerations are $\ddot{\underline{g}}_{N(m_N \times 1)}$ and $\ddot{\underline{g}}_{T(m_T \times 1)}$. The terms m_N and m_T are the number of potentially active normal and tangential constraints while \underline{W}_N and \underline{W}_T are the constraint matrices relating system derivatives $\dot{\underline{u}}$ to the relative accelerations $\ddot{\underline{g}}_N$ and $\ddot{\underline{g}}_T$ respectively. The matrices $\tilde{\underline{w}}_N$, $\tilde{\underline{w}}_T$, $\bar{\underline{w}}_N$ and $\bar{\underline{w}}_T$ arise due to prescribed motion in the system. Equation (3b) can now be written in form

$$\underline{M} \dot{\underline{u}} + \underline{A}_B^T \underline{\lambda}_B + (\underline{W}_N + \underline{\mathcal{H}}) \underline{\lambda}_N + \underline{W}_T \underline{\lambda}_T = \underline{K}. \quad (7)$$

In the above equation, the contact force has been segregated into normal ($\underline{\lambda}_N$) and tangential ($\underline{\lambda}_T$) components, while $\underline{\lambda}_B$ represents the generalized bilateral constraint forces. \underline{A}_B^T represents the bilateral constraint Jacobian and $\underline{\mathcal{H}}$ takes into account sliding friction as a function of the normal contact force $\underline{\lambda}_N$. In equation (7) there are n unknowns in the generalized accelerations $\dot{\underline{u}}$, m_B unknowns in the bilateral constraint forces $\underline{\lambda}_B$, m_N and m_T unknowns in the relative accelerations of the potential contacts $\ddot{\underline{g}}_N$ and $\ddot{\underline{g}}_T$ respectively. Similarly, there are an additional m_N and m_T unknowns associated with the corresponding unilateral constraint forces $\underline{\lambda}_N$ and $\underline{\lambda}_T$ resulting in a total of $n + m_B + 2(m_N + m_T)$ unknowns. Equations (5) and (7) along with the equations for bilateral constraints represented in equation (3c) provide $n + m_B + m_N + m_T$ equations. The remaining $m_N + m_T$ equations are provided by Signorini's Law or the unilateral contact conditions [3] given as

$$\ddot{\underline{g}}_N \geq \underline{0} \quad , \quad \underline{\lambda}_N \geq \underline{0} \quad , \quad \ddot{\underline{g}}_N^T \underline{\lambda}_N = \underline{0}. \quad (8)$$

Now one may proceed by treating the unilateral constraints as a set of bilateral constraints which are selectively made active or inactive [2, 19]. In this approach, all the individual contact states must be monitored at each time step. At this point a single transition in a contact state has an influence on all other contact states within the system, and may result

in the need for the simultaneous transition of additional contact states. Unfortunately, there is no *a priori* knowledge of what this appropriate system-wide contact state is, which makes a search for a valid new contact state set necessary. The worst case scenario results in an extremely expensive $O(2^{mu})$ combinatorial problem of determining a consistent set of contact states.

The $O(2^{mu})$ combinatorial problem can, to a significant degree, be sidestepped using a complementarity formulation to describe contact states. In this approach, the contact laws including all possible transitions like contact/detachment and slide/stiction are formulated as linear or non linear complementarity conditions [4] depending upon the contact features. The Coulomb's friction law then takes the well known form for a two dimensional contact which can be written as

$$0 \leq \dot{\underline{g}}_T^+ \perp \mu \underline{\lambda}_N + \underline{\lambda}_T \geq 0, \quad (9a)$$

$$0 \leq \dot{\underline{g}}_T^- \perp \mu \underline{\lambda}_N - \underline{\lambda}_T \geq 0. \quad (9b)$$

Where, the superscripts + and - denote the positive and negative direction of relative sliding. This model describes the stiction and sliding regimes in the following manner. When the frictional force is sufficiently large to prevent any motion, then we have $|\underline{\lambda}_T| < \mu \underline{\lambda}_N$ and $\dot{\underline{g}}_T = 0$, which clearly satisfy equations (9a) and (9b). When the body is sliding in the positive direction, $\dot{\underline{g}}_T^+ > 0$, $\dot{\underline{g}}_T^- = 0$ and $\underline{\lambda}_T = -\mu \underline{\lambda}_N$ which again satisfy the complementarity conditions given above. The case when the body is sliding in negative direction can similarly be explained.

This model can be extended into a 3D version based on the desired approximation of the friction cone. Thus equations (7) along with equations (8) and (9) corresponding to each contact can now be solved together as a complementarity problem using existing methods. However, solution to this problem is also potentially expensive for large and highly constrained systems. If an indirect method (e.g Lagrangian formulation) with relative coordinates is used in the formulation of equation of motion (7), then the solution of the system state derivative requires the decomposition of the system mass matrix $\underline{M}_{(n \times n)}$. This decomposition process by direct methods has an order- n^3 or $O(n^3)$ expense, where n is the number of generalized coordinates for the system. Additionally, each of the matrix blocks appearing as a coefficient matrix to $\{\underline{\lambda}_B^T, \underline{\lambda}_N^T, \underline{\lambda}_T^T\}$ are densely populated. As a result the overall computational cost associated with the formation and solution of the complementarity problem using a traditional indirect dynamics formulation as described above at each time step is $O(n^3 + nm^2 + m^3)$ with $m = m_B + m_N + m_T$. By comparison, if a full descriptor formulation [20] is used, then all the constraint forces appear explicitly and \underline{M} is effectively a block diagonal matrix and can be easily inverted. However in this case, m_B is very large and the matrix blocks involving \underline{A}_B appearing in equation (7) are of large dimension and often highly populated for heavily constrained systems. In such cases, one must often use the special sparse-stiff DAE solvers.

Given this undesirable growth in computational expense with problem size for articulated body systems, the cost of simulating large systems can quickly become prohibitive. The performance of the conventional complementarity based models is severely hampered for highly constrained systems, specially when the number of bilateral constraints in the systems

is much larger than the number of unilateral constraints in the systems. A combination of order- n methods for constrained multibody systems and complementarity methods can effectively address this issue.

3 Rigid Body Contact Model

In this section, the contact model for a single rigid body will be described. In section 4 this formulation will be extended to generalized multibody system in a DCA framework. The contact model used in this formulation is identical to the one described in [10, 14, 21] and is very briefly discussed here in an effort to make the paper more self contained.

The contact model consists of a set of equations and inequalities enforcing the Newton Euler equations of motion and kinematic non-penetration constraints for a rigid body with dry friction at the contacts. Consider a body with a spatial 6×6 mass matrix M . Let q and u retain their prior meaning, then the dynamics of this body is described by the equation

$$M(q)\dot{u} = F_a(q, u) + F_c(q, u). \quad (10)$$

Where F_a is the 6×1 vector of external/body forces which is completely known based on the state of the body and F_c is the unknown 6×1 force vector due to a unilateral constraint on the body. F_c consists of a normal contact force (λ_N) and a frictional force (λ_F) which can be nonzero only when the unilateral constraint is active. In the following discussion we would look at the complementarity conditions governing the contact force.

3.1 Friction Model

Typically for any body in space, there is a set of possible states it can take without interpenetrating with any solid object in its environment. Based on the knowledge of the state of the body and the interacting environment, it is possible to come up with a distance function $g_N = f(q)$, where q represents the generalized coordinates of the body, which is positive when there is no contact, equal to zero when there is a contact and negative when there is interpenetration. This is illustrated in figure 1. Points P and Q are located on the convex boundaries of the interacting bodies. Knowing the state of the system, the location of points P and Q can be computed such that the vector \vec{PQ} has the least possible magnitude [6]. Then $g_N = |\vec{PQ}|$. For a generalized 3D environment there are several techniques to compute the distance function $f(q)$ [22]. Here, we assume that a signed distance function is available in the form of existing softwares or methods and can be used directly.

Without considering the details of the solid modeling used for objects in space and the algorithms used to detect interpenetration, we simply state the interpenetration constraint on the body as $f(q) \geq 0$. When we encounter a situation where all the bodies under consideration are moving, the function $f(q)$ is dependent on the states of all the involved bodies. Since the interacting bodies are not fixed in space, an equal and opposite contact force is then applied on each of the interacting bodies when $f(q) = 0$.

Let λ_N denote the magnitude of the normal contact force acting at the point of contact. Then, for $f(q) > 0$ we have $\lambda_N = 0$. Similarly, for $\lambda_N > 0$ we get $f(q) = 0$. This can be compactly written in the complementarity form as

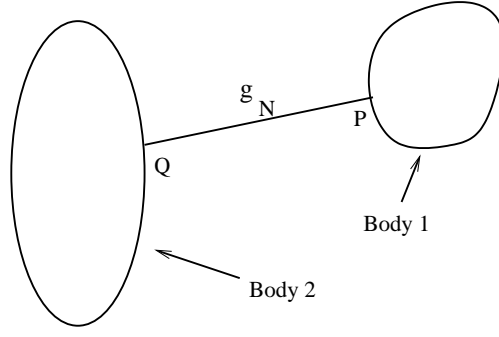


Figure 1: Proximal points between two convex bodies

$$0 \leq f(q) \perp \lambda_N \geq 0. \quad (11)$$

The corresponding frictional force (λ_F) acting on the body lies in the tangential plane at the point of contact and whose magnitude is constrained by the inequality $|\lambda_F| \leq \mu\lambda_N$, where μ is the coefficient of friction. In order to cast the contact model into an linear complementarity problem (LCP), we use a polygonal approximation (Figure 2) of the circular friction cone. In figure 2, \vec{n} denotes the unit normal vector at the point of contact and \vec{d}_i , $i = 1$ to η are the directions of vectors which positively span the space of possible frictional forces, η being the number of possible friction directions. Thus, if we have a vector \vec{v} in the space spanned by the set of vectors $\{\vec{d}_i\}$ and $\vec{d}_i \cdot \vec{v} \geq 0$ for all i , then $\vec{v} = \vec{0}$. The friction cone is approximated by the expression

$$\mathcal{F} = \{\lambda_N \vec{n} + \lambda_F \vec{\mathcal{D}}_c \mid \lambda_N \geq 0, \lambda_F \geq 0, e^T \lambda_F \leq \mu \lambda_N\}. \quad (12)$$

Here, the columns of $\vec{\mathcal{D}}_c$ are the vectors \vec{d}_i describing the possible directions of friction and $\lambda_F \in \mathfrak{R}^\eta$ is a vector of weights corresponding to each direction. μ is the coefficient of friction and $e = [1, 1, \dots, 1]^T \in \mathfrak{R}^\eta$. For isotropic friction models, \vec{d}_i would be a unit vector while for anisotropic models the magnitude of these vectors could vary.

3.2 Model Discretization

If h is the fixed time step of integration and t^l is the current time, then equation (10) can be discretized as

$$M \cdot (\mathcal{V}^{l+1} - \mathcal{V}^l) = h(F_a(q^l + hu^l/2, u^l) + \lambda_N \vec{n} + \lambda_F \vec{\mathcal{D}}_c), \quad (13a)$$

$$\mathcal{V}^l = G(q, t) \cdot u^l + \mathcal{V}_i(q, t), \quad (13b)$$

$$q^{l+1} - q^l = hu^{l+1}. \quad (13c)$$

Here, $h\lambda_N$ and $h\lambda_F$ are the impulses of the normal and frictional contact force over the time period from t^l to t^{l+1} . $G(q, t)$ is the mapping between the generalized speeds u and the spatial velocity \mathcal{V} of the body. $\mathcal{V}_i(q, t)$ refers to the velocity remainder term [23] which corresponds to the prescribed motion of the body. The goal here is to compute q^{l+1} and u^{l+1}

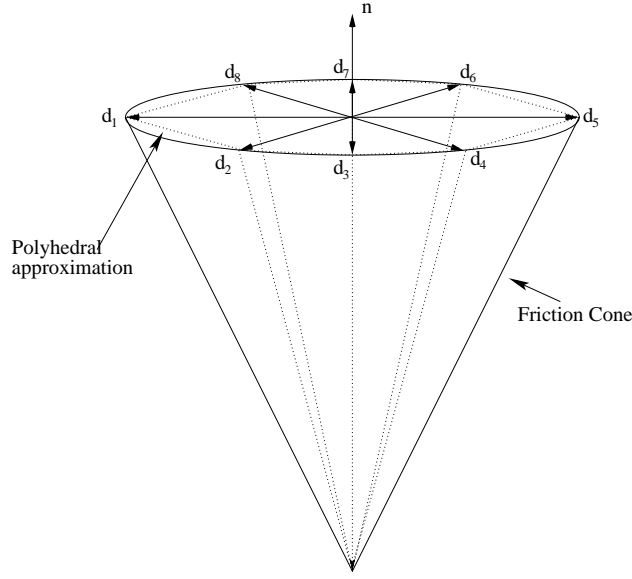


Figure 2: Polygonal approximation of the circular friction cone [10]

that satisfy this model and the maximum work inequality which will set the direction of the frictional force during a sliding contact. The set of complementarity conditions necessary to correctly model the frictional force and interpenetration constraints described earlier are given by

$$0 \leq f(q^{l+1}) \perp \lambda_N^{l+1} \geq 0, \quad (14a)$$

$$0 \leq \mathcal{S}^{l+1} e + \vec{\mathcal{D}}_c^T \cdot (\vec{v}_r^{l+1} + \frac{\delta g_T}{\delta t}) \perp \lambda_F^{l+1} \geq 0, \quad (14b)$$

$$0 \leq \mu \lambda_N^{l+1} - e^T \lambda_F^{l+1} \perp \mathcal{S}^{l+1} \geq 0. \quad (14c)$$

The additional variable \mathcal{S} introduced here approximates the magnitude of the relative contact velocity. In the case where there is no sliding and the frictional force is zero, \mathcal{S} can take any non-negative value and satisfy the model. However, in this particular case the value of \mathcal{S} has no physical meaning. \vec{v}_r is the relative contact velocity vector and is a function of the generalized speed u . $\frac{\delta g_T}{\delta t}$ represents the prescribed relative velocity vector between the interacting bodies in the tangential direction at the point of contact.

For most cases the distance function does not take a closed form expression. To get around this, a first order approximation for $f(q^{l+1})$ is used in equation (14a) which can be written as

$$f(q^{l+1}) = f(q^l) + h \vec{n} \cdot \vec{v}_r^{l+1} + \frac{\delta g_N}{\delta t} + \epsilon. \quad (15)$$

Here, $\frac{\delta g_N}{\delta t}$ accounts for the prescribed motion between the two bodies in the \vec{n} direction and ϵ is the first order error. Since we are currently dealing only with a single rigid body, the spatial relative contact velocity \vec{v}_r can be computed easily in terms of the q and u . In section 4.2.1, the paper will discuss the computation of \vec{v}_r for a general multibody system.

The complementarity conditions given in (14) cover separation, sliding and a rolling contact and have been described in more detail in [10, 14]. The complementarity condition (14a) enforces the non-penetration constraint while (14b) and (14c) ensure that the frictional force lies inside the linearized friction cone with the direction of frictional force acting on the body being approximately opposite to the direction of relative tangential sliding. The model in its current format is a mixed linear complementarity system. A pure LCP can be obtained in the following manner. Use equations (13a) and (13c) to express q^{l+1} and u^{l+1} in terms of the other unknowns and substitute in equation (14) to obtain a LCP. The contact model described in equation (14) is such that sufficient impulse is applied at the contact to prevent interpenetration within first order errors. If used in the current format, the model describes a purely inelastic contact.

A velocity restitution model [21] (Newton’s hypothesis) can be incorporated into this setup by additional complementarity constraints. Suppose an impact has occurred during time step t^{l-1} to t^l . This will be indicated by a non-zero normal impulse. The rebound velocity at time t^{l+1} will then be a fraction (coefficient of restitution ϵ_N) of the approach velocity at time t^{l-1} . The complementarity condition (14a) can then be replaced by the following

$$0 \leq \vec{n} \cdot (\vec{v}_r^{l+1} + \epsilon_N \vec{v}_r^{l-1}) \perp \lambda_N^{l+1} \geq 0. \quad (16)$$

An impulse restitution model [12] (Poisson’s hypothesis) can also be introduced if required by replacing equation (16) by the appropriate complementarity conditions. The implementation of either of the restitution models in a DCA framework is identical, albeit with different complementarity conditions. For the purpose of demonstrating the hybrid DCA-complementarity approach, velocity restitution model is included.

In this section the discussion was limited to a contact model for a single body. In the following section this will be extended to articulated multibody systems in a DCA framework.

4 DCA with Unilateral Constraints

The DCA is used to solve the forward dynamics problem for articulated multibody systems with open loops, closed loops or *ladder-type* topologies [15]-[17]. A DCA framework to model unilateral constraints can be used to decouple the bilateral and unilateral constraints in the multibody system. This results in an efficient formulation for classes of systems where the number of unilateral constraints is much less than the number of bilateral constraints. Such systems are encountered in robotics, molecular modeling and complex spacecraft design.

The basic idea of the DCA is to treat a larger multibody system by recursively assembling adjacent articulated bodies (subsystems) into larger encompassing subsystems. This idea is demonstrated in figure 3. At the finest level the individual bodies and/or sub-domains are represented by the individual leaves of the binary tree. These are referred to as the “leaf nodes”. Within an individual leaf node, all the dynamics of the node are in evidence. However, these leaf nodes have been modeled in such a way that from the outside the only dynamics in evidence is the apparent rigid-body motion of key points on the body boundary (referred to as “handles”) through which these nodes interact with their environment. These nodes are in turn be assembled into fictitious bodies (Intermediate nodes) as the procedure works down to produce the next lower level of the binary tree. This assembly is done in a

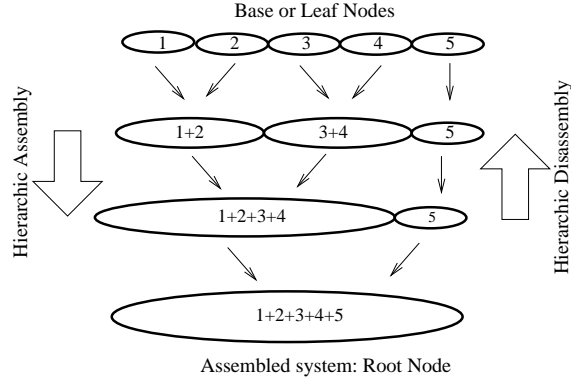


Figure 3: The hierarchic assembly and disassembly process using binary tree structure

similar manner for which the internal dynamics of the nodes remain invisible, while only the dynamics of the handles remain in evidence. This process is repeated in a recursive manner as one works downward through the associated binary tree representation until one reaches the root node of the tree. At this level the root node appears as a fictitious spatial rigid body with unknown joint accelerations and constraint forces at it's boundary/terminal handles. The resulting linear system of spatial equations for the root node provides as many equations as there are unknown joint accelerations and constraint forces and may thus be directly solved to obtain these values. The process is then reversed. The now known handle accelerations and joint forces are used to recursively disassemble the nodes into their component nodes, solving for the associated internal joint accelerations and constraint forces. The DCA then consists of two distinct processes, hierarchic assembly and disassembly which must be carried out at each temporal integration.

4.1 Hierarchic Assembly

Consider two bodies, k and $k + 1$ of any articulated system as shown in figure 4. The joint between these bodies is referred to as $J^{k/k+1}$. The two handles on body k corresponding to the locations H_1^k and H_2^k are associated with joints $J^{k-1/k}$ and $J^{k/k+1}$, respectively. Further the spatial acceleration of the handle H_i^k and the constraint force acting on this point will be denoted by the superscript k and subscript i .

In figure 4, F_u^k is the force acting on body k due to a unilateral constraint and consists of the normal contact force λ_N and frictional force λ_F . The assumption here is that the location of the impending or current contact is known. The equations of motion for body k using a spatial Newton-Euler formulation can be expressed as

$$M_0^k \mathcal{A}_0^k = \mathcal{F}_0^k, \quad (17a)$$

$$M_0^k = \begin{bmatrix} I_0^k & \mathcal{Z} \\ \mathcal{Z} & m^k \end{bmatrix}, \quad \mathcal{A}_0^k = \begin{bmatrix} \alpha_0^k \\ a_0^k \end{bmatrix}, \quad \mathcal{F}_0^k = \begin{bmatrix} \tau_0^k \\ f_0^k \end{bmatrix}. \quad (17b)$$

Here, the subscript “0” denotes the center of mass of the body, while superscript k indicates that the quantity is associated with body k . In equation (17), M_0^k is the 6×6 spatial inertia

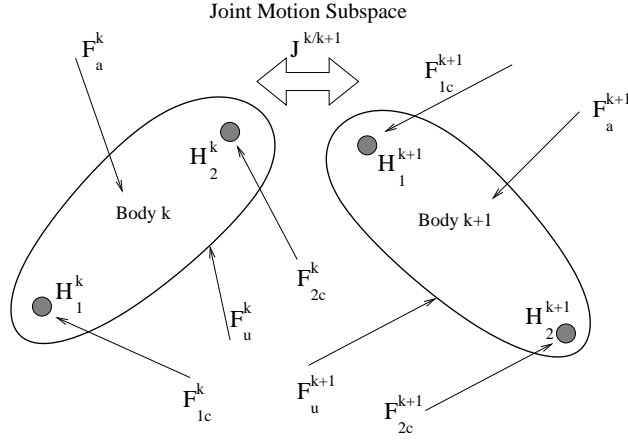


Figure 4: Representative bodies of a multibody system

matrix of k about the point “0” and is composed of the 3×3 inertia matrix I_0^k of body k about its center of mass, the 3×3 diagonal mass matrix m^k in which each diagonal element of the matrix is equal to the mass of body k , and 3×3 zero matrices \mathcal{Z} . The quantity \mathcal{A}_0^k is the 6×1 spatial acceleration associated with the center of mass of body k in the inertial reference frame N . This matrix is comprised of the 3×1 angular acceleration vector α_0^k of body k in N and the translational acceleration a_0^k of the body k mass center in N . Similarly, \mathcal{F}_0^k is the resultant spatial loads matrix associated with all loads (applied and constraint) acting on body k . This matrix is composed of the resultant torque τ_0^k acting on body k with the resultant force f_0^k acting on k with a line of action through the center of mass of k . Thus, if there are ν unilateral constraints acting on body k , equation (17a) can be written as

$$\mathcal{M}_0^k \mathcal{A}_0^k = S^{k_0/k_1} \mathcal{F}_{1c}^k + S^{k_0/k_2} \mathcal{F}_{2c}^k + \sum_{i=1}^{\nu} S_i^{k_0/k_{ui}} \mathcal{F}_{ui}^k + \mathcal{F}_a^k, \quad (18)$$

where

$$S^{k_0/k_i} = \begin{bmatrix} \mathcal{U} & r_{\times}^{k_0/k_i} \\ \mathcal{Z} & \mathcal{U} \end{bmatrix}_{6 \times 6}. \quad (19)$$

Here, \mathcal{U} is a 3×3 identity matrix. r^{k_0/k_i} refers to the position vector from point “0” to point i on body k . \mathcal{F}_{1c}^k and \mathcal{F}_{2c}^k are the unknown constraint loads acting on handles H_1^k and H_2^k respectively, and \mathcal{F}_a^k is the resultant of all the applied spatial loads acting on body k . \mathcal{F}_{ui}^k is the force due to i^{th} unilateral constraint and can be expressed in terms of λ_{Ni} and λ_{Fi} as

$$\mathcal{F}_{ui}^k = \begin{bmatrix} \mathcal{Z}_{3 \times 1} \\ \vec{n}_i^k \end{bmatrix}_{6 \times 1} \lambda_{Ni}^k + \begin{bmatrix} \mathcal{Z}_{3 \times \eta} \\ \mathcal{D}_{ci} \end{bmatrix}_{6 \times \eta} \lambda_{Fi}^k. \quad (20)$$

In equation (20), \vec{n}_i^k is the normal at the i^{th} point of contact, \mathcal{D}_{ci} is a $3 \times \eta$ matrix corresponding to η directions of friction as shown in figure 2 and λ_{Fi}^k is the $\eta \times 1$ vector of weights corresponding to each friction direction (See equation (12)). We also have a set of complementarity conditions (14a)-(14c) for each point of contact. Thus, equation (18)

along with ν complementarity conditions of the form (14a)-(14c) describe the dynamics of the single rigid body.

From equations (18) and (20), the expressions for the spatial acceleration of the joint handles of the body k can be written as

$$\mathcal{A}_1^k = \zeta_{11}^k \mathcal{F}_{1c}^k + \zeta_{12}^k \mathcal{F}_{2c}^k + \zeta_{13}^k + \sum_{i=1}^{\nu} (\zeta_{14i}^k \lambda_{Ni}^k + \zeta_{15i}^k \lambda_{Fi}^k), \quad (21a)$$

$$\mathcal{A}_2^k = \zeta_{21}^k \mathcal{F}_{1c}^k + \zeta_{22}^k \mathcal{F}_{2c}^k + \zeta_{23}^k + \sum_{i=1}^{\nu} (\zeta_{24i}^k \lambda_{Ni}^k + \zeta_{25i}^k \lambda_{Fi}^k). \quad (21b)$$

The above equation set is henceforth referred to as the two-handle equations of motion for body k . \mathcal{A}_1^k and \mathcal{A}_2^k are then the spatial accelerations of body k for handles H_1^k and H_2^k , respectively. The terms \mathcal{F}_{1c}^k , \mathcal{F}_{2c}^k and λ_{Ni}^k , λ_{Fi}^k are the unknown bilateral and unilateral constraint loads respectively acting on the body k . Similarly, the two-handle equations of motion for body $k+1$ can be written as

$$\mathcal{A}_1^{k+1} = \zeta_{11}^{k+1} \mathcal{F}_{1c}^{k+1} + \zeta_{12}^{k+1} \mathcal{F}_{2c}^{k+1} + \zeta_{13}^{k+1} + \sum_{i=1}^{\nu} (\zeta_{14i}^{k+1} \lambda_{Ni}^{k+1} + \zeta_{15i}^{k+1} \lambda_{Fi}^{k+1}), \quad (22a)$$

$$\mathcal{A}_2^{k+1} = \zeta_{21}^{k+1} \mathcal{F}_{1c}^{k+1} + \zeta_{22}^{k+1} \mathcal{F}_{2c}^{k+1} + \zeta_{23}^{k+1} + \sum_{i=1}^{\nu} (\zeta_{24i}^{k+1} \lambda_{Ni}^{k+1} + \zeta_{25i}^{k+1} \lambda_{Fi}^{k+1}). \quad (22b)$$

In the above discussion, it was assumed that there are ν unilateral constraints acting on each body. In subsequent discussion, we assume that there is a single unilateral constraint acting on body k . This is done for ease of describing the method and is not limiting in any way. Although the formulation for multiple unilateral constraints is not explicitly given, the implications of the same in are discussed in the following sections.

Equations (21) and (22) can then be rewritten in the following form for a single unilateral constraint acting on body k as

$$\mathcal{A}_1^k = \zeta_{11}^k \mathcal{F}_{1c}^k + \zeta_{12}^k \mathcal{F}_{2c}^k + \zeta_{13}^k + \zeta_{14}^k \lambda_N^k + \zeta_{15}^k \lambda_F^k, \quad (23a)$$

$$\mathcal{A}_2^k = \zeta_{21}^k \mathcal{F}_{1c}^k + \zeta_{22}^k \mathcal{F}_{2c}^k + \zeta_{23}^k + \zeta_{24}^k \lambda_N^k + \zeta_{25}^k \lambda_F^k, \quad (23b)$$

$$\mathcal{A}_1^{k+1} = \zeta_{11}^{k+1} \mathcal{F}_{1c}^{k+1} + \zeta_{12}^{k+1} \mathcal{F}_{2c}^{k+1} + \zeta_{13}^{k+1}, \quad (23c)$$

$$\mathcal{A}_2^{k+1} = \zeta_{21}^{k+1} \mathcal{F}_{1c}^{k+1} + \zeta_{22}^{k+1} \mathcal{F}_{2c}^{k+1} + \zeta_{23}^{k+1}. \quad (23d)$$

To combine bodies k and $k+1$, one uses the kinematic relationship between the spatial accelerations \mathcal{A}_2^k and \mathcal{A}_1^{k+1} given by the equation

$$\mathcal{A}_1^{k+1} = \mathcal{A}_2^k + P^{k/k+1} \dot{u}^k + \dot{P}^{k/k+1} u^k. \quad (24)$$

$P^{k/k+1}$ is the $6 \times f^k$ matrix of the *free-modes of motion* [24], permitted by the f^k degree-of-freedom joint $J^{k/k+1}$ with each column of the matrix $P^{k/k+1}$ being synonymous with the spatial *partial velocities* [23] of the joint. u^k and \dot{u}^k are the $f^k \times 1$ matrices of relative

generalized speeds and accelerations for the joint between bodies k and $k + 1$. We define a matrix $D^{k/k+1}$ as the orthogonal complement of $P^{k/k+1}$. $D^{k/k+1}$ is a $6 \times (6 - f^k)$ matrix containing the constrained degrees of freedom for the joint $J^{k/k+1}$. Based on these definitions one gets the relationship

$$D^{k/k+1T} \cdot P^{k/k+1} = 0. \quad (25)$$

Premultiplying equation (24) by $D^{k/k+1T}$ and using the relationship (25) one obtains the following.

$$D^{k/k+1T} \mathcal{A}_1^{k+1} = D^{k/k+1T} (\mathcal{A}_2^k + \dot{P}^{k/k+1} u^k). \quad (26)$$

From Newton's third law, we have $\mathcal{F}_{1c}^{k+1} = -\mathcal{F}_{2c}^k$. Substituting equations (23b) and (23c) in equation (26), the expression for \mathcal{F}_{1c}^{k+1} in terms of the unknown constraint forces can be obtained in the following form.

$$\mathcal{F}_{1c}^{k+1} = \mathcal{C}_1 \mathcal{F}_{1c}^k + \mathcal{C}_2 \mathcal{F}_{2c}^{k+1} + \mathcal{C}_3 + \mathcal{C}_4 \lambda_N^k + \mathcal{C}_5 \lambda_F^k. \quad (27)$$

Substituting equation (27) into equations (23a) and (23d) the two-handle equation for the combined body can be obtained in the following form.

$$\mathcal{A}_1^k = \xi_{11} \mathcal{F}_{1c}^k + \xi_{12} \mathcal{F}_{2c}^{k+1} + \xi_{13} + \xi_{14} \lambda_N^k + \xi_{15} \lambda_F^k, \quad (28a)$$

$$\mathcal{A}_2^{k+1} = \xi_{21} \mathcal{F}_{1c}^k + \xi_{22} \mathcal{F}_{2c}^{k+1} + \xi_{23} + \xi_{24} \lambda_N^k + \xi_{25} \lambda_F^k. \quad (28b)$$

This process can now be repeated for all the bodies in the system. Adjacent bodies are coupled together in a hierarchic fashion until we have a single assembly for the entire multibody system as shown in figure 3. It should be noted that if all the bodies in the multibody system have a unilateral contact force associated with them, then all these unknown forces are present in the two-handle equation of the assembled system. If one assumes that in a multibody system with n bodies, there is a single unilateral constraint active on body k , then the two-handle equations of the assembled system can be written as

$$\mathcal{A}_1^1 = \gamma_{11}^{1:n} \mathcal{F}_{1c}^1 + \gamma_{12}^{1:n} \mathcal{F}_{2c}^n + \gamma_{13}^{1:n} + \gamma_{14}^{1:n} \lambda_N^k + \gamma_{15}^{1:n} \lambda_F^k, \quad (29a)$$

$$\mathcal{A}_2^n = \gamma_{21}^{1:n} \mathcal{F}_{1c}^1 + \gamma_{22}^{1:n} \mathcal{F}_{2c}^n + \gamma_{23}^{1:n} + \gamma_{24}^{1:n} \lambda_N^k + \gamma_{25}^{1:n} \lambda_F^k. \quad (29b)$$

Here $1 : n$ denotes the system root assembly containing bodies 1 through n .

4.2 Time-stepping and Hierarchic Disassembly

A general multibody system may have different constraints on the boundary handles. For example, we can have a system with a closed kinematic loop and position constraints on each of the boundary handles or we can have an open loop with unconstrained boundary handles or a combination of the two. In the absence of unilateral constraints, the general procedure to solve equation (29) is described in [15]-[17]. Here, the solution scheme with unilateral constraint on a single body in an articulated multibody system is discussed.

The goal is to discretize the two-handle equations of motion and cast them into a form similar to that of equation (13a). In equation (29), if λ_N and λ_F are treated as parameters, then for different constraints on the terminal handles of the assembly, there are equal number of unknowns and equations. Following the solution scheme described in [15]-[17] it is possible to reduce equation (29) to the following form.

$$\mathcal{A}_1^1 = \kappa_{11}^{1:n} + \kappa_{12}^{1:n} \lambda_N^k + \kappa_{13}^{1:n} \lambda_F^k, \quad (30a)$$

$$\mathcal{A}_2^n = \kappa_{21}^{1:n} + \kappa_{22}^{1:n} \lambda_N^k + \kappa_{23}^{1:n} \lambda_F^k. \quad (30b)$$

For a fixed time step h and current time t^l , equation (30) can be discretized in terms of the spatial velocities \mathcal{V}_1^1 and \mathcal{V}_2^n as

$${}^{l+1}\mathcal{V}_1^1 - {}^l\mathcal{V}_1^1 = h(\kappa_{11}^{1:n} + \kappa_{12}^{1:n} \lambda_N^k + \kappa_{13}^{1:n} \lambda_F^k), \quad (31a)$$

$${}^{l+1}\mathcal{V}_2^n - {}^l\mathcal{V}_2^n = h(\kappa_{21}^{1:n} + \kappa_{22}^{1:n} \lambda_N^k + \kappa_{23}^{1:n} \lambda_F^k). \quad (31b)$$

4.2.1 The Mixed Complementarity Problem

The discretized two-handle equation of the assembly given in (31) along with the complementarity conditions given in equation (14) form our mixed complementarity problem (MCP). In case we had Ξ unilateral constraints acting on the system, the contact force corresponding to each constraint would turn up in the discretized two-handle equation of the assembly. Also, we would have a set of complementarity conditions of the form (14) for each contact.

The problem is however not yet fully specified. To use the complementarity conditions, one must express ${}^{l+1}\vec{v}_r^k$ which is the relative velocity for body k at the point of contact at time step $l+1$ in terms of ${}^{l+1}\mathcal{V}_1^1$ and ${}^{l+1}\mathcal{V}_2^n$. This can be done in the following manner. As a first step, one may assemble all the bodies connected via bilateral constraints which do not have any unilateral constraints acting on them to obtain sub-systems $1 : (k-1)$, k and $(k+1) : n$ as shown in figure 5. The resulting sub-systems are then assembled to obtain the two-handle equations of motion for the root node. Computing ${}^{l+1}\mathcal{V}_1^k$ (or ${}^{l+1}\mathcal{V}_2^k$) is an intermediate step in expressing ${}^{l+1}\vec{v}_r^k$ as a function of ${}^{l+1}\mathcal{V}_1^1$ and ${}^{l+1}\mathcal{V}_2^n$. To this end, one partially initiates the disassembly process.

The hierarchic disassembly process involves computing the spatial velocities of all the intermediate bodies at time step t^{l+1} from the known quantities of the terminal bodies. For example, the solution of the assembly from body k and body $k+1$ gives us λ_N^k , λ_F^k , \mathcal{F}_{1c}^k , \mathcal{F}_{2c}^{k+1} , \mathcal{A}_1^k and \mathcal{A}_2^{k+1} . Substituting these values in equations (23a) and (23d) one can solve for the constraint force \mathcal{F}_{2c}^k and \mathcal{F}_{1c}^{k+1} . From these and equations (23b) and (23c), one can then solve for the joint accelerations \mathcal{A}_2^k and \mathcal{A}_1^{k+1} . Thus the disassembly process can continue in a similar recursive fashion until all the joint constraint forces and spatial accelerations of all the bodies are known.

The identical process can be used to obtain an explicit function of the form ${}^{l+1}\mathcal{V}_1^k = \varsigma^1({}^{l+1}\mathcal{V}_2^n) + \varsigma^2(q^l, u^l)$ (or equivalently ${}^{l+1}\mathcal{V}_2^k = \varsigma^1({}^{l+1}\mathcal{V}_1^1) + \varsigma^2(q^l, u^l)$). ς depends upon the order in which the bodies were assembled during the hierarchic assembly process. From this, one gets the expression for \vec{v}_r^k in the form ${}^{l+1}\vec{v}_r^k = \chi^1({}^{l+1}\mathcal{V}_2^n, q^l, u^l) + \chi^2(q^l, u^l)$.

Then, the resulting MCP is to find x such that, $y = Ax + b$, where

$$y = [0 \ 0 \ \vartheta_1 \ \vartheta_2 \ \vartheta_3]^T, \quad (32a)$$

$$x = [{}^{l+1}\mathcal{V}_1^1 \ {}^{l+1}\mathcal{V}_2^n \ h\lambda_N \ h\lambda_F \ \mathcal{S}]^T, \quad (32b)$$

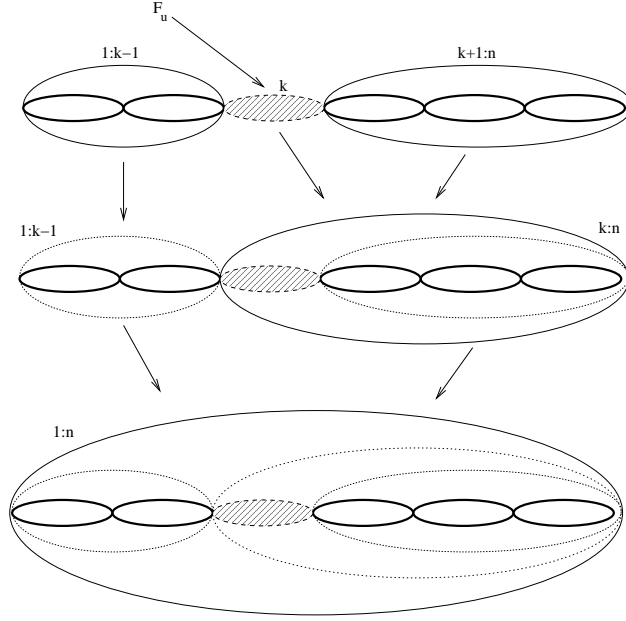


Figure 5: Assembly process for a unilateral constraint on body k

$$b = \begin{bmatrix} {}^l\mathcal{V}_1^1 + h\kappa_{11}^{1:n} \\ {}^l\mathcal{V}_2^n + h\kappa_{21}^{1:n} \\ \frac{f(q^l)}{h} + \hat{n}\chi^2 + \frac{\delta g_N}{\delta t} + \Delta_N \\ \frac{\delta g_T}{\delta t} \\ 0 \end{bmatrix}, \quad (32c)$$

$$A = \begin{bmatrix} -\mathcal{U}_{6 \times 6} & \mathcal{Z}_{6 \times 6} & \kappa_{12}^{1:n} & \kappa_{13}^{1:n} & \mathcal{Z}_{6 \times 1} \\ \mathcal{Z}_{6 \times 6} & -\mathcal{U}_{6 \times 6} & \kappa_{22}^{1:n} & \kappa_{23}^{1:n} & \mathcal{Z}_{6 \times 1} \\ \hat{n}^T \chi^1 & & 0 & \mathcal{Z}_{1 \times \eta} & 0 \\ \mathcal{D}_c^T \chi^1 & & \mathcal{Z}_{\eta \times 1} & \mathcal{Z}_{\eta \times \eta} & e \\ \mathcal{Z}_{1 \times 12} & & \mu & -e^T & 0 \end{bmatrix}, \quad (32d)$$

along with the complementarity condition

$$0 \leq \begin{bmatrix} \vartheta_1 \\ \vartheta_2 \\ \vartheta_3 \end{bmatrix} \perp \begin{bmatrix} h\lambda_N \\ h\lambda_F \\ \mathcal{S} \end{bmatrix} \geq 0. \quad (32e)$$

Here, \mathcal{U} and \mathcal{Z} are identity and zero matrices, respectively, with dimensions given by the subscripts. Also, $\Delta_N = \epsilon_N \vec{v}_r^{l-1} \cdot \vec{n}$ and is non-zero only if an impact has occurred in the previous time-step. The matrix χ^1 acts either on ${}^{l+1}\mathcal{V}_1^1$ or ${}^{l+1}\mathcal{V}_2^n$. Consequently, it is expected to be a dense 3×6 matrix. However, in equation (32c), it is represented as a 3×12 matrix with the understanding that either the first six or the last six columns consists only of zeros. The complementarity relation given in (32e) is equivalent to (14) with ϑ_i representing the L.H.S of the complementarity conditions. The advantage of this method is that the size of the MCP is independent of the number of bilateral constraints in the system and depends only on the number of unilateral constraints. The disadvantage is that matrix χ^1 , is expected

to be dense, but is still small compared to what one would find using more conventional complementarity methods on real engineering applications.

The other possible approach in formulating the MCP involves appending the equation of spatial velocity for body k to the discretized equations of motion forming a larger MCP. The matrices y and x for our complementarity problem $y = Ax + b$, can then be written as

$$y = \begin{bmatrix} 0 \\ 0 \\ 0 \\ \vartheta_1 \\ \vartheta_2 \\ \vartheta_3 \end{bmatrix}, \quad x = \begin{bmatrix} {}^{l+1}\mathcal{V}_1^1 \\ {}^{l+1}\mathcal{V}_2^n \\ {}^{l+1}\mathcal{V}_1^k \\ h\lambda_N \\ h\lambda_F \\ \mathcal{S} \end{bmatrix}. \quad (33)$$

In this case, χ^1 is a sparse matrix of the form $\begin{bmatrix} \bar{r} \times & \vdots & \mathcal{U} \end{bmatrix}_{3 \times 6}$ and acts on the spatial velocity vector ${}^{l+1}\mathcal{V}_1^k$, while χ^2 is a zero matrix. $\bar{r} \times$ is the cross-matrix for position vector \bar{r} from the point of impending contact to the handle H_1^k and \mathcal{U} is a 3×3 identity matrix.

Thus, for different kinematic constraints on the boundary handles, at the end of assembly step we have the two-handle discretized equations of motion for the assembled body along with the unknown contact forces acting on body k . These discretized two-handle equations of motion are in required form as described in section 3.1. Additionally, the complementarity conditions described in equation (14) for the contact and frictional force apply directly to the unilateral constraint on body k . These can now be solved for using any MCP solver (e.g PATH solver [25]) to obtain the values of ${}^{l+1}\mathcal{V}_1^1$, ${}^{l+1}\mathcal{V}_2^n$ and contact impulses $h\lambda_N$ and $h\lambda_F$. Knowing these values, the hierarchic disassembly process can now be initiated to obtain the spatial velocities of all the bodies at time t^{l+1} .

4.2.2 Efficiency of the Method

There are three distinct steps in the proposed method of modeling unilateral constraints. The first step is the hierarchic assembly of the multibody system to give the discretized two-handle equations of motion for the root node. These equations along with the complementarity conditions of the form (14a)-(14c) for each unilateral constraint results in a MCP. The second step involves solving this MCP giving the spatial velocities of the terminal handles at the end of the current time step. The third step is the hierarchic disassembly process which gives the spatial velocities of all the intermediate bodies at the end of the current time step. The hierarchic assembly and disassembly can be done in $O(n)$ [15]-[17] for serial implementation, where n is the number of generalized coordinates for the system. The second step is potentially the most expensive of the three steps and dictates the overall speed of the simulation.

The MCP solvers rely on numerical methods to generate a solution and consequently the speed of the MCP solver is directly affected by the size of the complementarity problem and the structure of the involved matrices. In the following discussion, the authors provide an estimate of the size of the MCP that must be solved at each time step.

For each unilateral constraint, two additional unknowns ($\lambda_N \in \mathfrak{R}^1$ and $\lambda_F \in \mathfrak{R}^n$) are introduced in the assembled two-handle equations of the system satisfying the complementarity conditions described in (14). For a multibody system with Ξ unilateral constraints,

the number of unknowns that appear in the MCP can be estimated as follows. The discretized two-handle equations of motion have ${}^{l+1}\mathcal{V}_1^1$, ${}^{l+1}\mathcal{V}_2^m$, λ_{N_i} and λ_{F_i} ($i = 1$ to Ξ) as the unknowns. The spatial velocities result in 12 unknowns and λ_{N_i} contributes Ξ unknowns. If one assumes that at each contact, there are η possible directions of frictional force, then each λ_{F_i} contributes η unknowns. Thus, the total number of unknowns corresponding to weights of friction directions are $\Xi\eta$. There are an additional Ξ unknowns corresponding to \mathcal{S}_i in the complementarity conditions. Thus the total number of unknowns are then $12 + 2\Xi + \Xi\eta$ of which $2\Xi + \Xi\eta$ correspond to the complementarity conditions and the remaining correspond to the discretized two-handle equations of motion.

As was seen in section 4.2.1, there are two distinct ways to formulate the MCP in a DCA context. The first approach results in a smaller MCP with a dense 3×6 matrix χ_i^1 corresponding to each contact. In this case, the size of the MCP is $12 + 2\Xi + \Xi\eta$.

The second approach results in a larger MCP with a sparse 3×6 matrix χ_i^1 . This approach involves appending the spatial velocity of the handles of the bodies with unilateral constraints to the discretized two-handle equations of motion for the assembly. The spatial velocity of each body with a unilateral constraint adds an additional 6 unknowns. Thus, the size of the MCP in this case is $12 + 6\mathcal{B}_u + 2\Xi + \Xi\eta$, where \mathcal{B}_u is the number of bodies with unilateral constraints. We included only the number of bodies rather than the number of unilateral constraints in computing the size of MCP, since the relative contact velocity (\vec{v}_r), for all the unilateral constraints acting on the same body, can be computed from the spatial velocity of any handle on that body.

The size of the MCP in the traditional complementarity based approach to model unilateral constraints is directly dependent on the number of generalized coordinates and bilateral constraints in the system. For example, if one considers a multibody system with n generalized coordinates, then the traditional approach [11] results in a MCP with n equations which must be solved along with the complementarity conditions corresponding to each contact. To form a pure LCP, requires an inversion of $n \times n$ mass matrix.

For the proposed method, the size of the MCP is dependent on the approach used to compute the relative contact velocity \vec{v}_r and is independent of the number of generalized coordinates or bilateral constraints in the system. The first approach results in a smaller MCP of size $12 + 2\Xi + \Xi\eta$ but with denser matrices χ_i^1 . The second approach results in a larger MCP of the size $12 + 6\mathcal{B}_u + 2\Xi + \Xi\eta$ but with more sparse matrices χ_i^1 . The other possibility is to form a pure LCP. This can be done by expressing the unknowns ${}^{l+1}\mathcal{V}_1^1$ and ${}^{l+1}\mathcal{V}_2^n$ in terms of λ_N and λ_F using equation (31) and substituting the result in equation (32). As can be clearly observed, forming a pure LCP does not require any additional matrix inversions as is the case for conventional complementarity based methods [10, 12, 14].

The significant advantage of this method is the efficient treatment of the bilateral constraints and decoupling them from the unilateral constraints in the system. This is achieved by first assembling all the bodies which do not have any unilateral constraints on them into fictitious bodies. However, for multibody systems involving a possible unilateral constraint on all the bodies, this approach does not give any additional advantage over the existing methods.

4.3 Velocity Jump on Impact

While a unilateral constraint is inactive, the system's behavior is unaffected by the constraint. However, when the unilateral constraint becomes active, the constraint's presence is felt as an impulsive load applied to the system for the purpose of instantaneously enforcing the constraint. This impulsive load necessarily results in instantaneous velocity jumps which may pervade the system, depending on system kinematics. These velocity jumps are precisely of the nature one would expect to arise due to an impact in a system of bodies connected via bilateral constraints. Here, the authors briefly describe how the proposed method always computes the correct velocity jump across all the bodies, given the constraint impulse applied to the system. In the following discussion one assumes that the joint motion map does not change over the integration time step for the entire system. The more general case for discontinuous changes in rigid bodies has been discussed in [26].

The two-handle equations of motion for body k (See Eq. 23a, 23b) can be written in the discretized form

$$\Delta\mathcal{V}_1^k = \zeta_{11}^k \mathcal{I}_{1c}^k + \zeta_{12}^k \mathcal{I}_{2c}^k + \zeta_{13}^k + \zeta_{14}^k \mathcal{I}_N^k + \zeta_{15}^k \mathcal{I}_F^k, \quad (34a)$$

$$\Delta\mathcal{V}_2^k = \zeta_{21}^k \mathcal{I}_{1c}^k + \zeta_{22}^k \mathcal{I}_{2c}^k + \zeta_{23}^k + \zeta_{24}^k \mathcal{I}_N^k + \zeta_{25}^k \mathcal{I}_F^k. \quad (34b)$$

where $\mathcal{I} = \int \mathcal{F} dt \approx \mathcal{F} \Delta t$, is the impulse required for the instantaneous imposition of the constraint. During the assembly process, the method combines the bodies k and $k+1$ connected via a kinematic joint by eliminating the constraint force \mathcal{F}_{2c}^k . This is done using the fact that $\mathcal{F}_{2c}^k = -\mathcal{F}_{1c}^{k+1}$ and the kinematic relationship between \mathcal{A}_2^k and \mathcal{A}_1^{k+1} described in equation (24). One notes that the pairs $(\mathcal{I}, \mathcal{F})$ and $(\Delta\mathcal{V}, \mathcal{A})$ lie in the same joint free-modes of motion subspace as long as the joint motion map does not change over the integration time step. Consequently, if one uses an impulse-momentum formulation for each body described in equations (34a, 34b), the hierarchic assembly and disassembly processes remain unaltered.

From the above discussion, it is clear that if equation (34) was used for the leaf nodes, then the assembled two-handle equations of the root node are in fact the discretized form of equation (29) and can be written as

$$\Delta\mathcal{V}_1^1 = \gamma_{11}^{1:n} \mathcal{I}_{1c}^1 + \gamma_{12}^{1:n} \mathcal{I}_{2c}^n + \gamma_{13}^{1:n} + \gamma_{14}^{1:n} \mathcal{I}_N^k + \gamma_{15}^{1:n} \mathcal{I}_F^k, \quad (35a)$$

$$\Delta\mathcal{V}_2^n = \gamma_{21}^{1:n} \mathcal{I}_{1c}^1 + \gamma_{22}^{1:n} \mathcal{I}_{2c}^n + \gamma_{23}^{1:n} + \gamma_{24}^{1:n} \mathcal{I}_N^k + \gamma_{25}^{1:n} \mathcal{I}_F^k. \quad (35b)$$

Knowing the kinematic constraints on the boundary handles of the system, \mathcal{I}_{1c}^1 and \mathcal{I}_{2c}^n can be eliminated from (35) to obtain the equations for $\Delta\mathcal{V}_1^1$ and $\Delta\mathcal{V}_2^n$ in a form identical to that of equation (31).

The MCP in equation (32) must be solved at each time step. The solution to this MCP ensures that equation (31) is satisfied for the computed impact and frictional impulses. The impulse due to unilateral constraint on body k was already accounted for while writing it's two-handle equation of motion. Consequently, the correct velocity jump $\Delta\mathcal{V}$ for each body is computed as one works their way recursively through the binary-tree disassembly process.

5 Numerical Examples

The algorithm is demonstrated using the example of a free falling spatial double pendulum as shown in figure 6. Body A and body B are connected via a spherical joint at point P_2 .

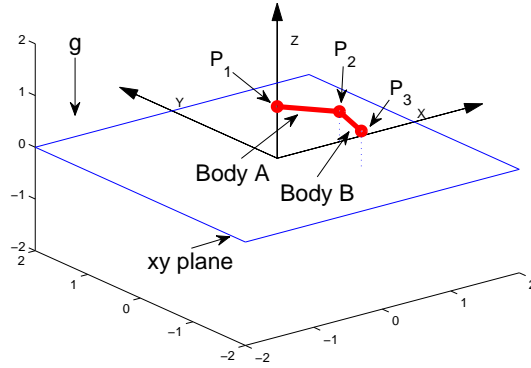


Figure 6: Unilateral constraint is defined between the xy plane and point P_1 on body A

A unilateral constraint is defined between the xy plane and point P_1 on body A . Gravity acts along negative z direction. Fixed parameters of the system are as follows. Length and mass of the two bodies are $L_a = L_b = m_a = m_b = 1$. The inertia matrix for each body is $I_a = I_b = \text{diag}(1, 2, 3)$, where diag is a diagonal matrix with diagonal elements listed in parentheses. The spatial orientation of the bodies is modeled using relative body fixed *Euler-123* transformations.

5.1 Inelastic Contact

For the validation of the model, the following two cases are studied. The orientation vector for the two bodies are set as $q_a = [0, 2, 0]$ and $q_b = [2, 0, 0]$. The system is released from rest with zero initial velocity and with point P_1 located at $(x, y, z) = (0, 0, 1)$.

In the first simulation, the coefficient of friction between the plane xy and point P_1 is set to zero, or $\mu = 0$. There are no external forces acting on the system in x and y directions. Consequently, one would expect the drift in x and y coordinates of the center of mass of the system to lie within integration errors. One expects that the slope of the indicated drift to be proportional to the integration step size, due to its direct effect on the temporal integrator accuracy. This is precisely what is seen in figure 7. The time-stepping method implements a first order integration scheme and consequently the errors are proportional to the time step. During the separation regime, the errors are significantly lower since the system behaves like a single rigid body falling under gravity.

To compare our results with an Autolev model of the system (See figure 8), the spatial orientation of the system is retained but with point P_1 located at $(x, y, z) = (0, 0, 0)$. Coefficient of friction is set to $\mu = 0.2$. The system is given an initial velocity of $V_x = V_y = 1$. The fixed time step used in our scheme is $\Delta T = 10^{-4}$. Plots 8(a) and 8(c) give the relative body fixed *Euler-123* angles generated by the time-stepping scheme and the Autolev model. Plots 8(b) and 8(d) show the absolute error in the orientation angles when compared with the Autolev model.

Next, to demonstrate the different regimes of motion, the case when the orientation vector

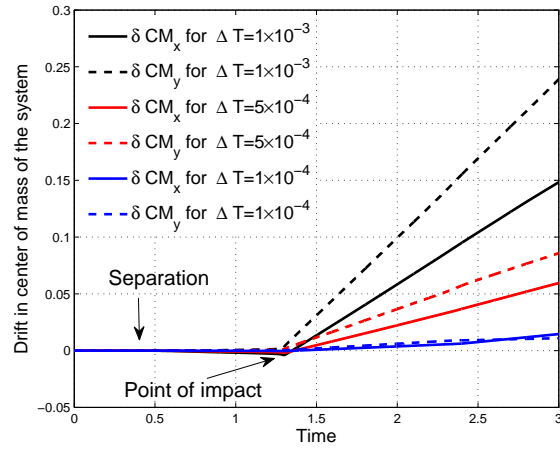
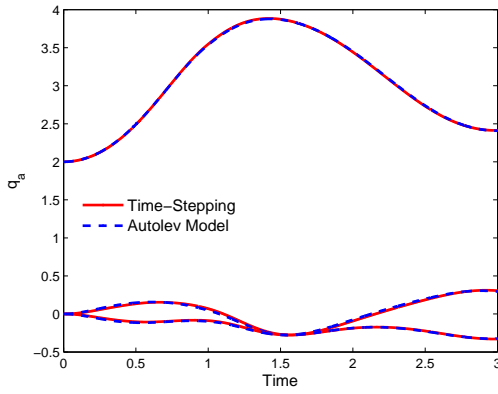
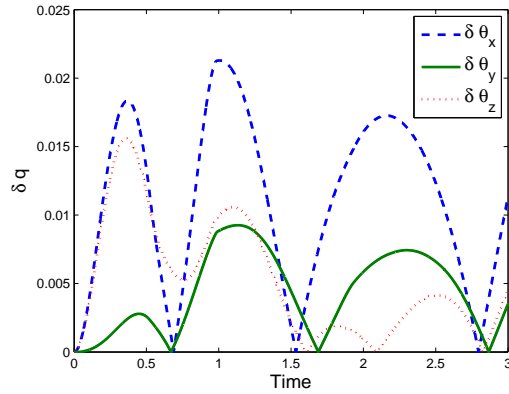


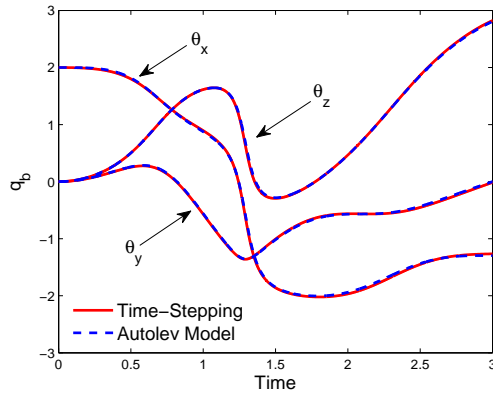
Figure 7: Drift in x and y coordinates of the center of mass of the double pendulum for $\mu = 0$



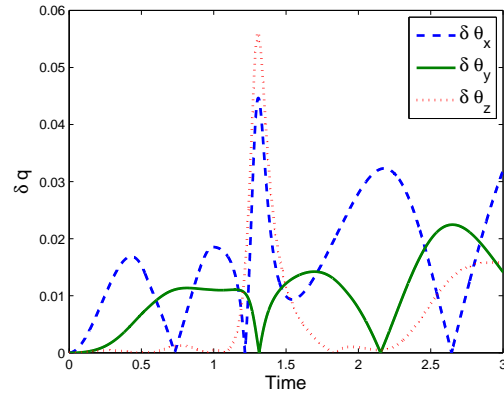
(a) Plot of body fixed relative *Euler-123* orientation angles for body A



(b) Absolute error in orientation angles for body A



(c) Plot of body fixed relative *Euler-123* orientation angles for body B



(d) Absolute error in orientation angles for body B

Figure 8: Comparison between the Time-Stepping scheme and Autolev Model

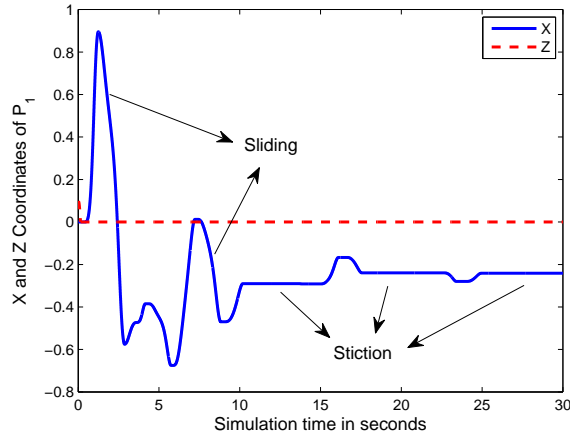


Figure 9: x and z coordinates of point P_1 for a planar (xz) double pendulum

for the two bodies are $q_a = [0, 1, 0]$ and $q_b = [0, 1, 0]$ is simulated. The system is released from rest with point P_1 located at $(x, y, z) = (0, 0, 0.1)$. The plot of the x and z coordinates of point P_1 with time is given in figure 9. Once, the point P_1 touches the xy plane, its z coordinate does not change and stays at 0. As the pendulum continues to oscillate, it loses energy due to the frictional force applied at point P_1 . During the simulation, when the frictional force acting on point P_1 lies within the friction cone, the pendulum enters the *stiction* regime and behaves like a planar double pendulum with a revolute joint at point P_1 . During the *slide* regime, the frictional force acting on P_1 lies on the boundary of the friction cone and pendulum continues to slide while losing energy.

5.2 Elastic Contact

Next, to demonstrate elastic contact, the coefficient of restitution is set to $\epsilon_N = 0.7$. The double pendulum is released from rest with point P_1 located at $(x, y, z) = (0, 0, 0.5)$ and the spatial orientation vector of two bodies being $q_a = [0, 1, 0]$ and $q_b = [0, 1, 0]$. Figure 10 gives the plot of the velocity of point P_1 for this planar elastic model.

As the simulation proceeds, the approach velocity of the point P_1 drops. The direct consequence of this is that there are multiple impacts occurring within a given time-step. These multiple impacts are not captured in the simulation. This is a characteristic of the velocity restitution model used in the simulation.

6 Conclusions

In this paper a *DCA-Complementarity* method is presented as means to efficiently model intermittent contact in certain classes of articulated constrained multibody systems. A complementarity based inelastic contact model and velocity restitution model was implemented in a DCA framework to yield a hybrid time-stepping scheme. The hybrid approach inherits all the properties of the contact model and the DCA framework makes the scheme ideal for application to systems with general topologies.

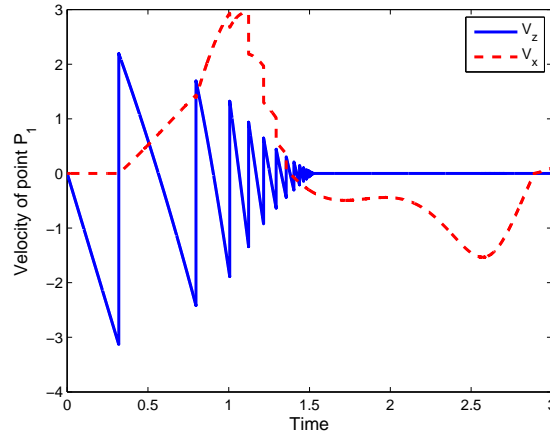


Figure 10: Elastic contact between point P_1 and xy plane, $\epsilon_N = 0.7$.

The complementarity contact model results in a MCP which must be solved at each time-step. In the complementarity based approaches to model multibody systems involving unilateral constraints, the speed of simulation depends primarily on the size of the MCP that must be solved at each time step. In the conventional approaches, the size of MCP is directly dependent on both, the number of bilateral and unilateral constraints. Also, formulating a pure LCP involves the inversion of a system-wide mass matrix. In the hybrid approach presented here, the size of the MCP depends only on the number of unilateral constraints in the system and formulating a pure LCP does not involve any matrix inversions. A LCP solver such as a PATH solver [25], can be used to solve the discretized two-handle equation of motion at the root node along with the associated contact complementarity conditions.

An existing DCA code need only be modified to compute the additional multipliers corresponding to the contact forces λ_N^k and λ_F^k at each contact. This can be done at the body level. During the assembly and disassembly process, one needs to keep track of these additional multipliers introduced due to the unilateral constraints. The two-handle equations of motion are formed at the leaf node and the assembly-disassembly process proceeds in a hierarchical fashion. This gives the analyst an option of serial or parallel implementation for the assembly-disassembly process.

The proposed method is expected to be more efficient than conventional complementarity based time stepping schemes for applications involving a large number of bilateral constraints and relatively fewer unilateral constraints (e.g certain robotics applications, bonding and/or docking of protein molecules) and the DCA framework for formulating equations of motion, makes it adequate for analyzing highly constrained systems involving unilateral constraints.

Acknowledgment

This work was supported by NSF Grant Number 0555174. The authors gratefully acknowledge this support.

References

- [1] Loetstedt, P., 1982, “Mechanical systems of rigid bodies subject to unilateral constraints,” *SIAM Journal of Applied Mathematics*, **42**(2), pp. 281–296.
- [2] Pereira, M. S. and Nikravesh, P., 1996, “Impact dynamics of multibody systems with frictional contact using joint coordinates and canonical equations of motion,” *Nonlinear Dynamics*, **53**, pp. 53–71.
- [3] Pfeiffer, F., 2003, “The idea of complementarity in multibody dynamics,” *Archive of Applied Mechanics*, **72**(11-12), pp. 807–816.
- [4] Trinkle, J., Pang, D., Sudarsky, S., and Lo, G., 1997, “On dynamic multi-rigid-body contact problems with coulomb friction,” *Zeitschrift fuer angewandte mathematik und mechanik*, **77**(4), pp. 267–279.
- [5] Barhorst, A., 1998, “On modelling variable structure dynamics of hybrid parameter multibody systems,” *Journal of Sound and Vibration*, **209**(4), pp. 571–592.
- [6] Pfeiffer, F. and Glocker, C., 2000, “Multibody dynamics with unilateral constraints, CISM courses and lectures no. 421,” International Centre for Mechanical Sciences. Springer.
- [7] Pfeiffer, F. G., 2001, “Applications of unilateral multibody dynamics,” *Royal Society of London Philosophical Transactions Series A*, **359**.
- [8] Moreau, J. J., 1988, “Unilateral contacts and dry friction in finite freedom dynamics,” *Non-Smooth Mechanics and Applications. CISM Courses and Lectures*, Springer Verlag, **302**.
- [9] Barhorst, D., 1993, “Issues in computing contact forces for non-penetrating rigid bodies,” *Algorithmica*, Springer New York, **10**(2-4), pp. 292–352.
- [10] Stewart, D. E. and Trinkle, J. C., 1996, “An implicit time-stepping scheme for rigid body dynamics with inelastic collisions and coulomb friction,” *International Journal of Numerical Methods in Engineering*, **39**, pp. 2673–2691.
- [11] Glocker, C. and Pfeiffer, F., 1995, “Multiple impacts with friction in multibody systems,” *Nonlinear Dynamics*, **7**, pp. 471–497.
- [12] Pfeiffer, F. and Glocker, C., 1996, “Multibody dynamics with unilateral contacts,” *Wiley Series in Nonlinear Sciences*. Wiley, New York.
- [13] Pfeiffer, F. G., 2003, “Unilateral multibody dynamics,” *Multiscale Computational Engineering*, **1**, pp. 311–326.
- [14] Stewart, D. E. and Trinkle, J. C., 1996, “An implicit time-stepping scheme for rigid body dynamics with inelastic collisions and coulomb friction,” *International Journal for Numerical Methods in Engineering*, **39**(15), pp. 2673–2691.

- [15] Featherstone, R., 1999, “A divide-and-conquer articulated body algorithm for parallel $o(\log(n))$ calculation of rigid body dynamics. part 1: Basic algorithm,” *International Journal of Robotics Research*, **18**(9), pp. 867–875.
- [16] Featherstone, R., 1999, “A divide-and-conquer articulated body algorithm for parallel $o(\log(n))$ calculation of rigid body dynamics. part 2: Trees, loops, and accuracy,” *International Journal of Robotics Research*, **18**(9), pp. 876–892.
- [17] Mukherjee, R. M. and Anderson, K. S., 2007, “Orthogonal complement based divide-and-conquer algorithm for constrained multibody systems,” *Nonlinear Dynamics*, **48**(1-2), pp. 199–215.
- [18] Cottle, R. W., Pang, J. S., and Stone, R. E., 1992, *The Linear Complementarity Problem*, Academic Press.
- [19] Haug, E. J., Wu, S. C., and Yang, S. M., 1986, “Dynamics of mechanical systems with coulomb friction, stiction, impact and constraint addition, deletion,” *Mechanism and Machine Theory*, **i, ii& iii**(21), pp. 401–425.
- [20] Schwertassek., R., 1994, “Reduction of multibody simulation time by appropriate formulation of the dynamics system equations,” *Computer-Aided Analysis of Rigid and Flexible Mechanical Systems*, NATO ASI, pp. 447–482.
- [21] Anitescu, M., 2003, “A fixed time-step approach for multi-body dynamics with contact and friction,” Tech. Rep. ANL/MCS-P1034-0303, Mathematics and Computer Science Division, Argonne National Laboratory, Argonne, Illinois.
- [22] Mirtich, B., 1996, “Impulse-based dynamic simulation of rigid body systems,” PhD thesis, University of California, at Berkeley, Department of Electrical Engineering and Computer Science.
- [23] Kane, T. R. and Levinson, D. A., 1985, *Dynamics: Theory and Application*, McGraw-Hill, NY.
- [24] Roberson, R. E. and Schwertassek, R., 1988, *Dynamics of Multibody Systems*, Springer-Verlag, Berlin.
- [25] Ferris, M. C. and Munson, T. S., 1999, “Interfaces to path 3.0: Design, implementation and usage,” *Computational Optimization and Applications*, **12**(1-3), pp. 207–227.
- [26] Mukherjee, R. M. and Anderson, K. S., 2007, “Efficient methodology for multibody simulations with discontinuous changes in system definition,” *Multibody System Dynamics*, **18**(2), pp. 145–168.